Published in final edited form as:
J Immunol. 2010 May 1; 184(9): 5141–5150. doi:10.4049/jimmunol.0903413.

Francisella Acid Phosphatases Inactivate the NADPH Oxidase in Human Phagocytes

Nrusingh P. Mohapatra[*,†], **Shilpa Soni**[*,†], **Murugesan V. S. Rajaram**[*,†], **Pham My-Chan Dang**[‡,§], **Tom J. Reilly**[¶], **Jamel El-Benna**[‡,§], **Corey D. Clay**[*,†], **Larry S. Schlesinger**[*,†,1], and **John S. Gunn**[*,†,1]

[*]Department of Molecular Virology, Immunology and Medical Genetics, Center for Microbial Interface Biology, The Ohio State University, Columbus, OH 43210

[†]Division of Infectious Diseases, Department of Internal Medicine, The Ohio State University, Columbus, OH 43210

[‡]INSERM, U773, Centre de Recherche Biomédicale Bichat Beaujon CRB3

[§]Université Paris 7 Denis Diderot, UMRS 773, Paris, France

[¶]Department of Veterinary Pathobiology and Veterinary Medical Diagnostic Laboratory, University of Missouri, Columbia, MO 65211

Abstract

Francisella tularensis contains four putative acid phosphatases that are conserved in *Francisella novicida*. An *F. novicida* quadruple mutant (AcpA, AcpB, AcpC, and Hap [ΔABCH]) is unable to escape the phagosome or survive in macrophages and is attenuated in the mouse model. We explored whether reduced survival of the ΔABCH mutant within phagocytes is related to the oxidative response by human neutrophils and macrophages. *F. novicida* and *F. tularensis* subspecies failed to stimulate reactive oxygen species production in the phagocytes, whereas the *F. novicida* ΔABCH strain stimulated a significant level of reactive oxygen species. The ΔABCH mutant, but not the wild-type strain, strongly colocalized with $p47^{phox}$ and replicated in phagocytes only in the presence of an NADPH oxidase inhibitor or within macrophages isolated from $p47^{phox}$ knockout mice. Finally, purified AcpA strongly dephosphorylated $p47^{phox}$ and $p40^{phox}$, but not $p67^{phox}$, in vitro. Thus, *Francisella* acid phosphatases play a major role in intramacrophage survival and virulence by regulating the generation of the oxidative burst in human phagocytes.

Francisella tularensis has been classified by the Centers for Disease Control and Prevention as a category A pathogen. Inhalation of <10 CFU of *F. tularensis* subspecies *tularensis* (hereafter *F. tularensis*) can have fatal consequences (1). *F. tularensis* can enter and multiply in a wide range of host cell types (2–9); however, in vivo, its primary target is the macrophage (10). *F. tularensis* enters host macrophages by asymmetric pseudopod loops, and this uptake is dependent on serum complement and host cell receptors, including C3, mannose, and scavenger (3,11–13). After entering the host cell, the bacterium arrests maturation of the phagosome, and the phagosome is transiently acidified. This acidification is reported to be essential for the subsequent escape of *F. tularensis* into the cytosol of the macrophage (14,

Address correspondence and reprint requests to Dr. Larry S. Schlesinger and Dr. John S. Gunn, The Ohio State University Biomedical Research Tower, Room 1006, 460 West 12th Avenue, Columbus, OH 43210-1214. larry.schlesinger@osumc.edu and gunn.43@osu.edu.
[1]L.S.S and J.S.G contributed equally to this work.

The online version of this article contains supplemental material.

Disclosures: The authors have no financial conflicts of interest.

15), but more recent work has contradicted this (15,16). Eventually, the phagosomal membrane is compromised by unknown mechanisms, and the bacteria escape into the cytoplasm and replicate (15,17,18). Subsequently, it was reported that the bacteria re-enter the endocytic pathway by an autophagy-like process, residing in large multiple-membrane bound vesicles (17,19). Bacterial release from host cells is thought to occur following *Francisella*-induced apoptosis (20–22) and pyroptosis (21). However, the final stages of the intracellular cycle are not well understood.

The intracellular life cycle of *F tularensis* is complex, and the genes involved with all stages are not well understood. However, the key genes involved in *Francisella* survival in host cells are found on the *Francisella* pathogenicity island (FPI). This island contains 19 genes, and bioinformatic analysis revealed that the FPI encodes a putative type VI secretion system, similar to the systems involved in the virulence of *Pseudomonas aeruginosa* (23) and *Vibrio cholerae* (24). Genes within the FPI are regulated by MglA, SspA, PmrA, MigR, Hfq, and FevR (25–31). Transcriptional analysis indicated that many genes outside of the FPI are also affected by these regulators (27,30).

In addition to the FPI genes, *Francisella* acid phosphatase AcpA was shown to play a key role in intracellular survival in macrophages (19,32,33). Bioinformatic analysis revealed that *Francisella* carries four or five acid phosphatases in its genome, depending on the species. Deletion of *acpA* resulted in a strain that was more susceptible than wild-type (WT) *Francisella tularensis* subspecies *novicida* (*F. novicida*) to killing by human and murine macrophages and had decreased phosphatase activity (32). Additionally, the mutant showed a decreased ability to escape from the phagosome (32). Deletion of three additional acid phosphatases (AcpA, AcpB, AcpC, and Hap [ΔABCH]) in *F. novicida* resulted in an attenuated strain that was 100% protective against homologous challenge in the mouse model. This mutant did not escape from the macrophage phagosome (19). Transcriptional analysis demonstrated that AcpA and Hap expression are increased during the early stages of macrophage infection (19).

Human neutrophils play a key role in host defense against invading pathogens and are major effectors of the acute inflammatory response. In response to a variety of agents, neutrophils produce a large amount of superoxide anion (O_2^-), which is essential for bacterial killing and amplifies the inflammatory response (34,35). The NADPH oxidase complex is responsible for O_2^- production, and its activation is induced by receptor ligation and uptake of microbial pathogens or chemical or particulate stimuli, such as PMA, fMLP, or zymosan. NADPH oxidase induction in neutrophils or macrophages requires the translocation of phosphorylated $p47^{phox}$, $p40^{phox}$, $p67^{phox}$, and Rac1/2 from the cytoplasm to the phagosomal membrane (34). However, *F. tularensis* live vaccine strain (LVS) enters neutrophils without triggering the respiratory burst and inhibits NADPH oxidase assembly by an unknown mechanism (36). Earlier studies showed that purified AcpA isolated from *Francisella* inhibited the respiratory burst of fMLP-induced porcine neutrophils in vitro (33). This suggests that *Francisella* may alter the function of the NADPH oxidase complex in a manner involving acid phosphatase dephosphorylation of key cellular components. We show in this study that the *Francisella* acid phosphatases are required for inhibiting NADPH oxidase assembly and function and may do so by dephosphorylation of NADPH oxidase components. This process aids the intracellular survival and proliferation of the bacterium.

Materials and Methods

Isolation of human monocyte-derived macrophages and neutrophils for infection with Francisella spp

Using an Ohio State University-approved Institutional Review Board protocol, heparinized blood samples were collected from normal human donors. The heparinized blood samples from

normal human donors were diluted 1:1 with normal saline, and the fraction containing the PBMCs was obtained following centrifugation at 800 × *g* for 40 min at 20°C over a Ficoll-Hypaque density cushion (Amersham Biosciences, Piscataway, NJ). This fraction was diluted 1:1 with RPMI 1640, and the PBMCs were collected again by centrifugation. The cells were washed twice with RPMI 1640, resuspended in the same media, and counted in a hemocytometer. The cell numbers were adjusted to 2 ± 10^6 PBMCs/ml in RPMI 1640 containing 20% autologous human serum. The monocytes were allowed to differentiate into monocyte-derived macrophages (MDMs) by incubation for 5 d at 37°C in 5% CO_2 in sterile screw cap Teflon wells. PBMCs (MDMs plus lymphocytes) were recovered and resuspended in RPMI 1640 with 10% autologous serum, and MDMs were plated in 24-well tissue culture plates or on coverslips at a density of 2×10^6 cells/well in 0.5 ml culture media, resulting in 2×10^5 MDMs/monolayer. For the respiratory burst experiments, the MDMs were placed in monolayer culture at 10^5 cells/well in 0.2 ml culture media in 96-well plates. After 2 h of incubation at 37°C in 5% CO_2, nonadherent cells were removed by washing the monolayers three or four times with prewarmed RPMI 1640 and replenished with fresh culture medium with 10% autologous serum. For intramacrophage survival assays, MDMs were incubated for an additional 7 d in fresh culture medium with 20% autologous serum to stabilize the MDM monolayer prior to infection (37). Macrophages were incubated with *Francisella* at a multiplicity of infection (MOI) ~50:1, as described earlier (12). At various time points, macrophages were lysed with 0.05% SDS and plated on Chocolate II plates to enumerate the CFU. This lysis protocol does not result in death of the bacteria (38).

After PBMC separation on Ficoll-Hypaque, the RBC-containing pellet was further fractionated by dextran sedimentation to separate the neutrophils. Briefly, RBCs were diluted 1:1 with normal saline, and an equal amount of 3% dextran was added to sediment the RBCs. After 30 min incubation on ice, the top layer of cells was transferred to a new tube and centrifuged at 800 × *g* for 15 min to enrich for the neutrophils. The erythrocytes that remained in the cell pellet were lysed with sterile distilled water for 15 s, and an equal amount of HBSS (without calcium and magnesium ions) containing 0.9% normal saline was added to prevent the lysis of neutrophils. Neutrophils were separated by centrifugation at 800 × *g* for 5 min. The cell pellet was washed, resuspended in HBSS media, and kept on ice for experimentation.

Growth and opsonization of Francisella spp

F. novicida U112, Δ*acpA*, and ΔABCH mutants were routinely cultured, as previously described (19). For phagocyte infection studies, *Francisella* strains were grown on Chocolate II plates overnight at 37°C and collected in HBSS buffer or RPMI 1640 (without phosphate). Cell density was determined spectrophotometrically at 600 nm; bacteria were opsonized with 50% autologous serum for 30 min at 37°C and subsequently washed three times with HBSS buffer to remove excess serum. *F. tularensis* subspecies *tularensis* (Schu S4, Type A) and *F. tularensis* subspecies *holarctica* (OR96-0246 from Biodefense and Emerging Infections Research Resources Repository, Type B, Manassas, VA) were cultivated and opsonized similarly to *F. novicida* strains. Opsonized *Francisella* were resuspended in appropriate buffer and kept on ice for experiments. Formalin-killed *Francisella* were prepared as described earlier (11). Zymosan beads were opsonized with 50% autologous serum, washed twice in HBSS without divalent cations, and kept on ice for the experiments.

Neutrophils (2×10^5 cells/well) were seeded onto human serum-coated 24-well plates in RPMI 1640, and *Francisella* were added at an MOI ~50:1. At time points ≤2 h postinfection, cells were washed and treated with 50 μg/ml gentamicin for 30 min, followed by washing with HBSS to remove the extracellular bacteria. Neutrophils were lysed by the addition of 0.05% SDS, and lysates were diluted in HBSS and plated on Chocolate II plates to enumerate the CFU.

Microscopy of *Francisella* association with and uptake by polymorphonuclear leukocytes

The association with and uptake of *F. novicida* and acid phosphatase mutants by polymorphonuclear leukocytes (PMNs) were performed as described earlier (12). In brief, neutrophils (2×10^5 cells/well) were seeded onto human serum-coated 24-well plates in RPMI 1640, and opsonized *Francisella* was added at an MOI ~50:1 and incubated for 10 min at 37° C in 5% CO_2. After incubation, the cells were washed extensively with RPMI 1640 to remove nonadherent bacteria and fixed in 3.5% paraformaldehyde without permeabilization or permeabilized after paraformaldehyde fixation with chilled 100% methanol for 15–30 s. The coverslips were washed and allowed to dry. Phagocyte-associated bacteria were visualized by indirect immunofluorescence microscopy. In this assay, PMNs on coverslips were incubated with a monoclonal mouse anti-*F. novicida* LPS primary Ab (Immuno-Precise Antibodies Limited, Victoria, British Columbia, Canada) and diluted 1:100 in blocking buffer composed of 20% human AB serum (Cambrex, East Rutherford, NJ) and 5% BSA (Sigma-Aldrich, St. Louis, MO) for 4 h at room temperature with gentle rotation. After being washed extensively, PMNs were incubated with Alexa Fluor 488-conjugated rabbit anti-mouse IgG (Molecular Probes, Eugene, OR) (diluted 1:1000 in blocking buffer) for 90 min at room temperature. Coverslips were mounted on glass slides. In all assays, the average number of bacteria per PMN on each coverslip was determined by counting a minimum of 200 cells per coverslip using an ×100 oil-immersion objective with a wide-bandwidth 570-nm dichroic mirror on a BX51 Olympus fluorescence microscope. Pictures were taken with a Color 3 digital camera (Olympus, Melville, NY). Triplicate coverslips were used for each test group. Attached bacteria were assessed by scoring nonpermeabilized PMNs, and total associated bacteria were assessed by scoring permeabilized PMNs. The number of bacteria taken up (internalized) was calculated by subtracting the number of attached bacteria from the number of associated bacteria.

Respiratory burst assays

Neutrophils (10^6/well) were added to human serum-coated microtiter wells in HBSS containing 10 mM glucose, 1% human serum albumin, and 50 μm luminol (Invitrogen, Carlsbad, CA) and left on ice for 15 min. Subsequently, serum-opsonized *Francisella* spp. were added at an MOI ~50:1. The microtiter plate was centrifuged at 400 × *g* for 2 min at 12° C to synchronize the infection. The relative amount of reactive oxygen species (ROS) generated by neutrophils over time was detected by measuring the luminescence by addition of luminol as a substrate in an ELISA reader (Spectramax M5, Molecular Devices, Sunnyvale, CA) after warming the cells to 37°C. In similar fashion, MDMs (10^5/well) were added in 0.2 ml culture media in 96-well plates. After 2 h of incubation at 37°C in 5% CO_2, nonadherent cells were removed by washing the monolayers three or four times with prewarmed RPMI 1640 and replenished with fresh culture medium containing 10% autologous serum, and the ROS production in MDMs in response to serum-opsonized *Francisella* (MOI ~50:1) was detected using the Diogenes enhanced luminescence system for superoxide detection (National Diagnostics, Atlanta, GA) with lucigenin as the substrate. Human serum-opsonized zymosan particles (MOI of 20:1) and PMA (200 nM) were used as positive controls for ROS production in neutrophils and MDMs. The inhibition of ROS production by *Francisella* spp. was tested by incubating phagocytes with *Francisella* for 10 min at 37°C prior to adding opsonized zymosan. ROS production was detected, as described above, in an ELISA reader.

ELISA to detect complement component deposition on Francisella strains

C5-depleted fresh human serum (CompTech, Tyler, TX) was used to evaluate complement component C3 deposition on *Francisella* strains, as described (39). Briefly, after preblocking microcentrifuge reaction tubes for 30 min in PBS with 0.1% HSA (ZLB Plasma, Boca Raton, FL), 3×10^8 bacteria/reaction were incubated in 10% or 50% serum for 30 min at 37°C. Reactions were stopped, and samples were washed twice in blocking buffer and once in PBS.

A total of 3×10^7 bacteria in suspension were added to medium-binding polystyrene wells in triplicate (Costar, Cambridge, MA) and left to dry overnight. Wells were blocked overnight at 4°C with 3% OVA. After extensive washing with PBS, primary Ab (goat antisera to human C3 diluted 1:10,000 in 0.3% OVA [Quidel, San Diego, CA]) was added for 1 h at room temperature. HRP-conjugated rabbit anti-goat IgG (H+L) Ab (Bio-Rad, Hercules, CA) diluted to 1:2000 was used as the secondary Ab and was added for 1 h at room temperature. Substrate was added for 10 min at room temperature (Bio-Rad), and the reaction was stopped with 2% oxalic acid. Absorbance at 415 nm was measured on a 96-well plate reader (Molecular Devices). Values obtained from reactions with heat-inactivated control serum were subtracted in each case.

Confocal microscopy

Neutrophils (10^6/well) were plated onto human serum-coated glass coverslips in HBSS in a 24-well plate. Serum-opsonized *Francisella* spp. were added at an MOI ~50:1, and the infection was synchronized at 12°C by centrifugation at 400 × *g* for 2 min. At different time intervals, coverslips were washed with HBSS to remove extracellular bacteria, and the cells were fixed with 3.5% paraformaldehyde for 30 min (40). After fixation, cells were washed three times with HBSS and permeabilized with chilled methanol for 15 s (41). Cells were washed again in HBSS and blocked in HBSS containing 20% normal human serum (Cambrex) and 5% BSA (blocking solution) for 2 h. Infected cells were treated with primary Ab consisting of mouse monoclonal anti-*F. novicida* (1:2000 dilution; Immunoprecise, Victoria, British Columbia, Canada) or mouse monoclonal anti-*F. tularensis* LPS (1:2000 dilution; Abcam, Cambridge, MA) and/or rabbit anti-$p47^{phox}$ Ab (1:1000 dilution; Molecular Probes) for 2 h in blocking solution. Coverslips were washed three times in blocking solution and secondary Ab [goat anti-mouse Alexa Fluor 488 or donkey anti-rabbit Alexa Fluor 546, 1:1000 dilution (Invitrogen)] was added for 1 h. Coverslips were washed and mounted with Prolong anti-fade reagent (Invitrogen) and viewed with a Zeiss 510 META confocal microscope. Resting neutrophils or cells activated with 200 nM PMA for 5 min were used as negative and positive controls, respectively. Using the same protocol, ~10^5 human MDMs in monolayer culture on coverslips were incubated with serum-opsonized *F. novicida* at an MOI ~50:1 to determine the colocalization of the bacterium with $p47^{phox}$ by confocal microscopy. Slides were examined using an ×63 oil-immersion objective on a Zeiss 510 META laser-scanning confocal microscope (Carl Zeiss Microimaging, Thornwood, NY). Quantification of colocalization of the *F. novicida* acid phosphatase mutants with $p47^{phox}$ at different time intervals was achieved by counting 1000 infected cells from triplicate coverslips in three independent experiments. Several attempts to perform colocalization experiments with Abs to gp91 and $p40^{phox}$ were unsuccessful because the rabbit anti-$p40^{phox}$ and rabbit anti-gp91 Abs did not recognize these NADPH oxidase components well.

Isolation and infection of bone marrow-derived macrophages from $p47^{phox}$ knockout mice

All of the mouse experiments were performed according to animal protocols approved by The Ohio State University. C57BL/6 WT and $p47^{phox}$ knockout (C57BL/6 background) mice were used in this study (generously provided by Dr. Chandan Sen, Ohio State University) (42). Three mice from each group were sacrificed, and the bone marrow-derived macrophages (BMDMs) were obtained from cultures of bone marrow stem cells, as previously described (43). In brief, the marrow was flushed from femurs with supplemented DMEM containing 10% FCS. The marrow plugs were disrupted into single-cell suspensions and cultured at a cell density of 1×10^6 nucleated cells/ml in 100-mm polystyrene tissue culture dishes containing 20 ml DMEM supplemented with 10% L cell-conditioned medium, 10% FCS. After 2 d of incubation at 37°C in 5% CO_2, the nonadherent cells were decanted. The remaining adherent monolayers were supplemented with fresh media, and cells were harvested after 2 d using cold HBSS buffer. $P47^{phox+/+}$ and $p47^{phox-/-}$ BMDMs were incubated with *F. novicida* strains at an MOI ~50:1.

At 30 min or 2 h postinfection, cells were washed twice and incubated with 50 μg/ml gentamicin for 30 min at 37°C and 5% CO_2. The cells were subsequently washed twice and replenished with fresh media containing 10 μg/ml gentamicin. Cells were lysed in 0.05% SDS at different time intervals and plated on Chocolate II agar plates to enumerate the CFU. Assays were performed in triplicate for each test group.

Detection of phosphorylated p40*phox* and *p47*phox in cell lysates of neutrophils and MDMs

Neutrophils (10^6/well) or MDMs (10^6/well) were added to a 12-well plate in RPMI 1640. Serum-opsonized *F. novicida* strains were added at an MOI ~50:1, and the infection was synchronized by centrifugation at 400 × *g* for 2 min at 12°C. At different time intervals, uninfected and infected cells were lysed in TN1 buffer (50 mM Tris [pH 8.0], 10 mM EDTA, 10 mM $Na_4P_2O_7$, 10 mM NaF, 1% Triton-X 100, 125 mM NaCl, 10 mM Na_3VO_4, 10 μg/ml each aprotinin and leupeptin). The cell lysates were boiled in Laemmli sample buffer, and equal amounts of proteins in the different test groups were separated by SDS-PAGE, transferred to a nitrocellulose membrane, and incubated with a primary Ab against phospho-p40*phox* (Cell Signaling Technology, Beverly, MA; 1:500 dilution in Tris-buffer saline with 5% milk) or phospho-p47*phox*, produced as described previously (1:1000 dilution) (44), overnight at 4°C. This was followed by a goat anti-rabbit HRP-conjugated secondary Ab (Bio-Rad; 1:1000 dilution for 2 h at room temperature) and development by ECL (Amersham/GE Healthcare Bio-Sciences, Piscataway, NJ). The ECL signal was quantified using a scanner and densitometry (Scion Image, Frederick, MD), as previously described (45).

In vitro phosphorylation and dephosphorylation of p47*phox*, p40*phox*, and p67*phox*

Recombinant p47phox, p67*phox*, and p40*phox* (5 μg each) were expressed in *Escherichia coli* using pGEX plasmids (gift from Bernard M. Babior, The Scripps Research Institute, La Jolla, CA) and then phosphorylated by active protein kinase C (PKC; Promega, Madison, WI) or AKT (Calbio-chem, San Diego, CA) in the presence of 1 μCi [^{32}P]-[γ]-ATP for 30 min using published protocols (46). The reaction was terminated by adding the same volume of 2× Laemmli sample buffer, boiled, and resolved by SDS-PAGE using 10% polyacrylamide gels. The separated proteins were transferred to a nitrocellulose membrane. Proteins were stained by ponceau red (data not shown), and [^{32}P]-labeled p47*phox*, p67*phox*, and p40*phox* were detected by a phosphoimager. The nitrocellulose areas containing [^{32}P]-labeled p47*phox*, p67*phox*, and p40*phox* were cut and incubated for 30 min at 37°C with polyvinylpyrrolidone, washed, and then incubated with 10 μg purified AcpA, AcpC, or Hap (47–50). All three proteins were separated and visualized by SDS-PAGE and showed functional acid phosphatase activity (data not shown). Supernatants containing released [^{32}P] were spotted onto a thin-layer cellulose plate (Merck, Whitehouse Station, NJ), and [^{32}P] was detected by autoradiography. To further confirm that the signal was not due to the release of the protein from the nitrocellulose, the supernatant was subjected to SDS-PAGE using 15% polyacrylamide gels and analyzed by autoradiography. Experiments were performed in duplicate and repeated twice.

Results

Production of ROS in human neutrophils and macrophages by *F. novicida* acid phosphatase mutants

Previous work showed that *F. tularensis* LVS is unable to stimulate an oxidative burst in infected human neutrophils and macrophages (36,51). In addition, acid phosphatases of organisms, including *Francisella* spp., have been implicated in respiratory burst inhibition (33,52–55). To determine whether *F. novicida* acid phosphatase mutants are no longer able to suppress the respiratory burst in human phagocytes, we measured the generation of ROS in infected human neutrophils (30-min time course) and MDMs (60-min time course) using the luminescence probe, luminol or lucigenin, respectively. *F. novicida* induced minimal amounts

of ROS in neutrophils and macrophages (Fig. 1A, 1B), demonstrating that *F. novicida*, like *F. tularensis* LVS (36), does not generate significant ROS production. Similar inhibitory effects were observed with Type A *F. tularensis* SchuS4 (Fig. 1C, 1D). Formalin-killed *Francisella* subspecies effectively induced a respiratory burst in MDMs and neutrophils, suggesting that ROS suppression was an active process of live bacteria (Fig. 1). Opsonized zymosan and PMA stimulated the production of ROS in neutrophils and MDMs, as expected (Fig. 1). However, the addition of opsonized zymosan after MDM or PMN infection by *F. novicida* or Schu S4 dramatically reduced ROS induction compared with opsonized zymosan alone (Fig. 1), demonstrating that *Francisella* subspecies are able to suppress ROS production from human phagocytes.

Phagocytes infected with the Δ*acpA* mutant produced a small amount of ROS, which was particularly evident in MDMs. However, neutrophils and MDMs infected with the ΔABCH strain produced significantly higher levels of ROS, with an overall 28-fold increase in neutrophils at 30 min postinfection and a 5.5-fold increase in MDMs at 60 min postinfection versus infection with *F. novicida*. The magnitude of ROS production in MDMs was significantly less than that observed in neutrophils during *F. novicida* strain infections (compare vertical axis of Fig. 1A with Fig. 1B). The ΔABCH strain was complemented with a plasmid expressing *acpA* (19). Additional complementation was too difficult to pursue because of the multiple antibiotic resistances of the ΔABCH strain. The results demonstrate that expression of the plasmid-borne *acpA* in the ΔABCH mutant complemented and dramatically reduced the amount of ROS produced by this strain, but not to the level of the WT *F. novicida* strain (Supplemental Fig. 1). Thus, these data suggest that loss of acid phosphatases in *Francisella* spp. results in a failure to suppress the production of ROS.

The above experiments were repeated with the addition of diphenylene iodonium (DPI; flavoprotein inhibitor) 15 min prior to bacterial infection. Luminescence was completely abrogated in neutrophils and MDMs postinfection with all bacterial strains as well as with PMA and opsonized zymosan (data not shown).

To confirm that differences in cell association or uptake were not responsible for the observed disparity in ROS production between acid phosphatase mutants and WT *F. novicida*, strains were examined by microscopy upon infection of MDMs and neutrophils in the presence of various concentrations of autologous serum. No significant differences in cell association or uptake were observed (data not shown). Additionally, there were no differences in the deposition of the complement component C3, a central complement factor whose cleavage leads to the deposition of C3bi, a major opsonin, on the surface of the *F. novicida* WT strain or the acid phosphatase mutants (data not shown).

Decreased survival of *F. novicida* acid phosphatase mutants in human macrophages and neutrophils is associated with enhanced ROS production

The ΔABCH mutant of *F. novicida* was reported to have an impaired ability to replicate intracellularly in J774.1 murine and THP-1 macrophages (19). In this study, we measured CFU in neutrophils (15 and 30 min) and MDMs (30 and 60 min) infected with the Δ*acpA*, ΔABCH, and WT strains of *F. novicida* (Fig. 2). At 30 and 60 min postinfection of neutrophils and MDMs, respectively, there was a 19- and 46-fold decrease in survival of the ΔABCH versus the *F. novicida* WT strain (Fig. 2A, 2C). In the presence of DPI, the intracellular growth of WT *F. novicida*, Δ*acpA*, and ΔABCH strains was nearly identical up to 30 min postinfection in neutrophils and 60 min postinfection in MDMs (Fig. 2B, 2D). Although growth at these time points was nearly identical, a nearly 2-log increase in survival was noted in the presence versus the absence of DPI. This is likely due to functional bacterial killing by residual ROS production upon infection by the *F. novicida* WT strain (incomplete suppression of ROS

production). These results suggest that the reduction in intracellular growth in phagocytes seen with the mutant strains was due to the generation of ROS.

To confirm whether ROS production was responsible for the decreased survival of acid phosphatase-deficient strains, we examined the survival of *Francisella* acid phosphatase mutants in BMDMs isolated from p47^{phox} knockout mice. These mice were shown to be more susceptible than WT mice to infection by *F. tularensis* LVS (56), demonstrating a role of ROS in controlling bacterial dissemination and growth. WT and p47$^{phox-/-}$ BMDMs were incubated with *F. novicida* WT, Δ*acpA*, and ΔABCH strains, and the CFU were compared at different time points. At 12 h postinfection, the ΔABCH strain showed a slightly less than 3-log decrease in survival compared with the WT strain (Fig. 3A). This decrease was even greater at 24 h. The Δ*acpA* strain demonstrated intermediate survival, with a >1.5-log decrease in survival at 12 h postinfection and ~1-log decrease in survival at 24 h. In contrast, the *F. novicida* WT, Δ*acpA*, and ΔABCH strains grew equally well in infected BMDMs isolated from p47$^{phox-/-}$ mice (Fig. 3B). Thus, there is a strong correlation of intracellular survival with the induction of ROS by the NADPH oxidase. These data, combined with the results in the presence of DPI, provide strong evidence that the production of ROS in phagocytes by the NADPH oxidase is responsible for the reduced intracellular survival seen with the *F. novicida* acid phosphatase mutants.

Colocalization of *Francisella* with the NADPH oxidase complex component p47^{phox} in human neutrophils and macrophages

Assembly of a functional NADPH oxidase requires the translocation of cytosolic NADPH oxidase components p67^{phox}, p47^{phox}, and p40^{phox} to the membrane component cytochrome b_{558} (57). However, intracellular *F. tularensis* LVS did not induce ROS production or colocalize with NADPH complex subunits (36). We examined colocalization of p47^{phox} with bacteria in human neutrophils and MDMs to determine whether the *F. novicida*, Δ*acpA*, ΔABCH, and Type A *F. tularensis* subspecies *tularensis* associate with NADPH oxidase complex components.

Neutrophils adhered to serum-coated glass coverslips were incubated with *F. novicida*, Δ*acpA*, or ΔABCH strains. The colocalization of *F. novicida* with p47^{phox} was detected using confocal microscopy. Representative confocal micrographs of neutrophils infected with the *F. novicida* and ΔABCH strains at 30 min postinfection are shown in Fig. 4A. Neutrophils infected with the ΔABCH strain showed a maximum colocalization at 30 min postinfection; ~90% of the bacteria were colocalized with p47^{phox} (Fig. 4B). The Δ*acpA* mutant strain colocalized less extensively with p47^{phox} (Fig. 4B). The *F. novicida* WT strain colocalized with p47^{phox} poorly, reaching a maximum ~12% at 30 min postinfection (Fig. 4B). Similarly, the virulent Type A and Type B strains colocalized poorly with p47^{phox} in neutrophils (7% and 8.5%, respectively) and MDMs (5.5% and 6.5%, respectively) at 30 min postinfection (data not shown).

Similar to what was observed in neutrophils, the ΔABCH strain demonstrated marked colocalization with p47^{phox} in MDMs (representative confocal micrographs are shown at 60 min postinfection in Fig. 5A), with a maximum of nearly 48% colocalization at 60 min postinfection (Fig. 5B). The Δ*acpA* mutant showed an intermediate level of colocalization (Fig. 5B), whereas the WT *F. novicida* strain showed the least association with p47^{phox} over the time period studied, with a maximum of only ~8% colocalization observed at 60 min postinfection.

NADPH oxidase components show increased phosphorylation following infection with the ΔABCH mutant strain relative to *F. novicida* WT in neutrophils and macrophages

To determine whether the limited generation of NADPH oxidase-mediated ROS in response to WT *F. novicida* involved the phosphorylation state of NADPH complex subunits by the acid phosphatases, we first examined the phosphorylation of p47^{phox} and p40^{phox} during the course of infection. Neutrophils were infected with *F. novicida* strains; at different time intervals, cells were lysed, and the phosphorylation of p47^{phox} or p40^{phox} was detected by Western blotting using phospho-p40^{phox} and phospho-p47^{phox} Abs (Fig. 6). In neutrophils, infection by the ΔABCH strain resulted in a marked increase in phosphorylation of p47^{phox} within 15 min of infection compared with the WT strain (Fig. 6). Similarly, phosphorylation of p40^{phox} in neutrophils infected with the ΔABCH strain showed a dramatic increase within 15 min of infection compared with the WT strain. In addition, MDMs infected with the ΔABCH strain showed a steady increase in phosphorylation of p47^{phox} and p40^{phox} over the time course of the experiment, which was not observed with the WT strain (data not shown). The relative increase in p47^{phox} and p40^{phox} phosphorylation during infection of neutrophils and MDMs with the ΔABCH strain versus infection with the WT strain suggests that these NADPH complex components do not become phosphorylated by upstream kinases or are dephosphorylated in human phagocytes when infected with the WT, but not the ΔABCH, strain.

Direct dephosphorylation of p47^{phox} and p40^{phox} by AcpA

Activation of the NADPH oxidase complex depends upon the phosphorylation and subsequent translocation of the cytosolic components p40^{phox}, p47^{phox}, and p67^{phox} to the phagosomal membrane (58). Several studies reported that *phox* components are substrates for phosphorylation by PKCs, Akt, and p38 MAPK (46,59–63). In this study, we used active PKC and Akt to phosphorylate purified p47^{phox}, p40^{phox}, and p67^{phox} proteins in the presence of [^{32}P]-[γ]-ATP (60). The phosphorylated p47^{phox}, p40^{phox}, and p67^{phox} proteins were separated by SDS-PAGE and transferred to a nitrocellulose membrane. The [^{32}P]-labeled proteins were detected by a phosphoimager and autoradiography (Fig. 7A); all three proteins were strongly phosphorylated by the kinases. Membranes containing [^{32}P]-labeled p47^{phox}, p67^{phox}, and p40^{phox} proteins were incubated with purified *Francisella* AcpA, AcpC, or Hap proteins (purified AcpB was difficult to obtain and was not available). The supernatants containing the released [^{32}Pi] were spotted on thin layer cellulose plates and detected by autoradiography (Fig. 7B). Purified AcpA strongly dephosphorylated p47^{phox} and p40^{phox} but only weakly dephosphorylated p67^{phox}. In the presence of AcpC and Hap, p47^{phox} was dephosphorylated to a small extent, whereas none of the other phosphorylated *phox* proteins tested were dephosphorylated by these two acid phosphatases (Fig. 7B). To confirm that [^{32}Pi] release was not due to the complete release of the nitrocellulose membrane-bound proteins, the supernatant was subjected to SDS-PAGE and analyzed by autoradiography. These data demonstrated that [^{32}Pi] was released from the proteins (Fig. 7C, 7D). Thus, the results provide evidence that p47^{phox} and p40^{phox} can be directly dephosphorylated by the *Francisella* acid phosphatases, particularly the AcpA protein.

Discussion

F. tularensis LVS is unable to stimulate the production of an oxidative burst in infected human neutrophils and macrophages and survives within these host cells (36,51). We previously reported that *F. novicida* acid phosphatases play a major role in survival within phagocytic cells and in virulence, because the loss of four acid phosphatases (AcpA, AcpB, AcpC, and Hap) in *F. novicida* (ΔABCH) rendered it unable to survive within and escape from human and murine macrophage phagosomes (19). The ΔABCH strain was also attenuated in the mouse model of tularemia. In addition, purified AcpA was reported to block the generation of an oxidative burst in neutrophils (33). These data led us to investigate the connection between

acid phosphatases and ROS production in human neutrophils and macrophages as a potential mechanism for the observed decrease in virulence and intraphagocytic cell survival of the ΔABCH strain.

In this study, we extend the work with *F. tularensis* LVS (36,51) to show that *F. tularensis* subspecies *tularensis* SchuS4, *F. tularensis* subspecies *holarctica*, and *F. novicida* also suppress the production of ROS in human neutrophils, as well as within human macrophages. Interestingly, although the live organisms induced similar low levels of ROS, formalin killed *F. novicida* induced considerably more ROS than did formalin-killed *F. tularensis* SchuS4, suggesting that there may be something inherently different about the surfaces of these bacteria that affect the respiratory burst. In addition, we provide evidence that infection with the ΔABCH strain results in a significant induction of ROS, suggesting that the acid phosphatases directly or indirectly interfere with the oxidative burst and that increased ROS production is responsible for the killing of the ΔABCH strain within these phagocytes. Indeed, blocking the assembly and/or function of the NADPH oxidase complex with DPI or mutation of a critical cytosolic component (murine $p47^{phox-/-}$ macrophages) allowed for a WT level of survival of the ΔABCH strain in phagocytes. The loss of only AcpA in *F. novicida* produced an intermediate amount of ROS production in neutrophils and MDMs and resulted in intermediate survival, suggesting that it was a major, but not the only, acid phosphatase contributing to the observed ΔABCH strain phenotypes.

Assembly of the NADPH oxidase requires that cytosolic phosphorylated $p47^{phox}$ and $p40/p67^{phox}$ heterodimers associate to form $p47/p67/p40^{phox}$ heterotrimers prior to their membrane translocation and subsequent association with flavocytochrome b_{558} (64–67). Similar to what was observed with the *F. tularensis* LVS strain, the *F. novicida* WT strain did not significantly colocalize with the $p47^{phox}$ component of the NADPH oxidase complex in human neutrophils and macrophages. However, the ΔABCH strain, and to a lesser extent, the *acpA* mutant, significantly colocalized with the $p47^{phox}$ in human neutrophils and human MDMs, correlating with their observed levels of ROS induction.

Several other bacteria and parasites were shown to mediate exclusion or disruption of NADPH oxidase assembly or ROS production during phagocytosis (52–55,68–72). For example, *Helicobacter pylori* disrupts phagosomal NADPH oxidase targeting, because superoxide anions are released extracellularly instead of within the phagosomes, and these phagosomes do not contain $p47^{phox}$ or $p67^{phox}$ (73–75). *Leishmania* exclude NADPH oxidase cytosolic components $p47^{phox}$ and $p67^{phox}$ from phagosomes in a lipophosphoglycan-dependent fashion (68,69). In contrast, *Salmonella* excludes flavocytochrome b_{558} from the phagosomal membrane, thus preventing NADPH oxidase assembly (54,72). Finally, *Coxiella burnetii* produces an acid phosphatase that, similar to *Francisella*, inhibits ROS production from activated human neutrophils by an unknown mechanism (55).

Recently published work suggested that AcpA, AcpB, and AcpC do not play a role in the pathogenesis of the *F. tularensis* SchuS4 strain (using a triple mutant) (76). This is contrary to our previous finding with *F. novicida*, which demonstrated increased virulence defects upon the accumulation of *acp* deletions, culminating with a strong virulence defect for the ΔABCH strain (quadruple mutant) (19). Our ongoing work with the acid phosphatases (Acps) in *F. tularensis* SchuS4 (data not shown), coupled with the data presented in this study, suggests that the acid phosphatases play a role in *F. tularensis* SchuS4 pathogenesis but perhaps not to the same extent as observed in *F. novicida*.

The hypothesis we developed based on the data presented in this work states that the acid phosphatases collectively directly participate in the dephosphorylation of *phox* components and/or of their kinases, which inhibits NADPH oxidase assembly and ROS production. In

support of an effect on the upstream kinases, human MDMs infected with the ΔABCH strain have an increased level of p38 MAPK phosphorylation, but not Akt and Erk1/2, compared with the MDMs infected with *F. novicida* WT strain (data not shown). Further studies are required to fully understand the phosphorylation patterns of the upstream kinases, including p38 MAPK, during ΔABCH strain infection. To address the *phox* components directly, phosphorylation of $p47^{phox}$ was weak and phospho-$p40^{phox}$ was undetectable at early time points post-infection of human neutrophils with the *F. novicida* WT strain. However, ΔABCH strain infection resulted in a marked increase in the phosphorylation of these *phox* components. To determine whether the Acps had the capacity to directly dephosphorylate the *phox* components, phosphorylated $p40^{phox}$, $p47^{phox}$, and $p67^{phox}$ proteins were treated individually in vitro with three purified *Francisella* Acps. AcpA strongly dephosphorylated the $p40^{phox}$ and $p47^{phox}$ proteins, but dephosphorylated $p67^{phox}$ weakly, demonstrating specificity in this reaction. As opposed to the actions of AcpA, AcpC and Hap weakly dephosphorylated $p47^{phox}$ but not $p40^{phox}$ or $p67^{phox}$. Although AcpA demonstrated the most activity toward the *phox* components in the in vivo assay, the virulence data (19) and the data presented in this article (including the colocalization data with $p47^{phox}$) suggest that a combined effort of the phosphatases is required for a maximal effect toward ROS suppression. Thus, there are likely targets of these phosphatases beyond the *phox* components, such as upstream kinases mentioned above, that are necessary for proper NADPH oxidase activation.

The rapid kinetics of NADPH oxidase inactivation by *Francisella* spp., coupled with the location of the targeted *phox* components, provide a conceptual challenge to these findings. Thus, how might AcpA or the other acid phosphatases be able to mediate these effects? Several pieces of data support a role for the *Francisella* acid phosphatases in this process. We previously demonstrated that two of the acid phosphatases, AcpA and Hap, were induced 219- and 10-fold, respectively, at 2 h postinfection with THP-1 macrophages (19). This induction decreased over time, suggesting that the peak activation may be prior to the 2 h time point. In addition, AcpA is outer membrane-associated in logarithmically growing cells (19), and it has been described as a *Francisella*-secreted protein, although this has not been observed in all studies that have screened for secreted factors. An acid phosphatase of *Legionella pneumophila*, a pathogen that resembles *F. tularensis* in a number of ways, is also secreted (77). None of the other *Francisella* Acps were reported to be secreted in vitro, but nothing is known about the potential secretion of these *Francisella* Acps in vivo. Thus, we hypothesize that *Francisella* affects the phagocyte (e.g., kinase dephosphorylation) very soon after contact, which may be Acp dependent and independent. Early secretion/release of acid phosphatases within the phagosome, or after phagosomal escape, which was described to occur rapidly after phagocytosis (17,78), would result in a further reduction of the phosphorylation of *phox* components normally necessary for proper NADPH oxidase assembly and function. A less likely possibility is that the ΔABCH mutant uses an unknown receptor for phagocyte entry that is associated with a more robust oxidative burst than normally occurs following entry via CR3 and the mannose receptor, known receptors for *Francisella* WT strains (12). Additional molecular and biochemical characterization, including localization, of the *Francisella* acid phosphatases within host phagocytes will further define the mechanisms by which this bacterial pathogen evades an early innate immune response, allowing for bacterial colonization and disease progression. Targeted inhibition of these phosphatases could be a therapeutic strategy against *Francisella* infection.

Supplementary Material

Refer to Web version on PubMed Central for supplementary material.

Acknowledgments

We thank Dr. Chandan Sen for providing p47^{phox} knockout mice for this study. The authors also thank Dr. Francis Nano for guidance in the initial work on *Francisella* acid phosphatases.

This work was supported by the National Institutes of Health, National Institute of Allergy and Infectious Diseases Regional Center of Excellence for Biodefense and Emerging Infectious Diseases Research Program. We acknowledge membership within and support from the Region V Great Lakes Regional Center of Excellence (National Institutes of Health Award 2-U54-AI-057153).

References

1. Oyston PC. *Francisella tularensis*: unravelling the secrets of an intracellular pathogen. J Med Microbiol 2008;57:921–930. [PubMed: 18628490]
2. Anthony LD, Burke RD, Nano FE. Growth of *Francisella* spp. in rodent macrophages. Infect Immun 1991;59:3291–3296. [PubMed: 1879943]
3. Ben Nasr A, Haithcoat J, Masterson JE, Gunn JS, Eaves-Pyles T, Klimpel GR. Critical role for serum opsonins and complement receptors CR3 (CD11b/CD18) and CR4 (CD11c/CD18) in phagocytosis of *Francisella tularensis* by human dendritic cells (DC): uptake of *Francisella* leads to activation of immature DC and intracellular survival of the bacteria. J Leukoc Biol 2006;80:774–786. [PubMed: 16857732]
4. Lindemann SR, McLendon MK, Apicella MA, Jones BD. An in vitro model system used to study adherence and invasion of *Francisella tularensis* live vaccine strain in nonphagocytic cells. Infect Immun 2007;75:3178–3182. [PubMed: 17339345]
5. Shepard CC, Ribi E, Larson C. Electron microscopically revealed structural elements of *Bacterium tularense* and their in vitro and in vivo role in immunologic reactions. J Immunol 1955;75:7–14. [PubMed: 13242796]
6. Shepard CC. Nonacid-fast bacteria and HeLa cells: their uptake and subsequent intracellular growth. J Bacteriol 1959;77:701–714. [PubMed: 13664649]
7. Councilman WTS, Strong RP. Plague-like infections in rodents. Trans Assoc Am Physicians 1921;36:135–143.
8. Buddingh GJW, Womack FC. Observations on the infection of chick embryos with *Bacterium tularense, Brucella*, and *Pasteurella pestis*. J Exp Med 1941;74:213–222. [PubMed: 19871129]
9. Francis E. Microscopic changes of tularemia in the tick *Dermacentor andersoni* and the bedbug *Cimex lectularius*. Public Health Rep 1927;42:2763–2772. [PubMed: 19315112]
10. Fortier AH, Green SJ, Polsinelli T, Jones TR, Crawford RM, Leiby DA, Elkins KL, Meltzer MS, Nacy CA. Life and death of an intracellular pathogen: *Francisella tularensis* and the macrophage. Immunol Ser 1994;60:349–361. [PubMed: 8251580]
11. Clemens DL, Lee BY, Horwitz MA. *Francisella tularensis* enters macrophages via a novel process involving pseudopod loops. Infect Immun 2005;73:5892–5902. [PubMed: 16113308]
12. Balagopal A, MacFarlane AS, Mohapatra N, Soni S, Gunn JS, Schlesinger LS. Characterization of the receptor-ligand pathways important for entry and survival of *Francisella tularensis* in human macrophages. Infect Immun 2006;74:5114–5125. [PubMed: 16926403]
13. Schulert GS, Allen LA. Differential infection of mononuclear phagocytes by *Francisella tularensis*: role of the macrophage mannose receptor. J Leukoc Biol 2006;80:563–571. [PubMed: 16816147]
14. Santic M, Asare R, Skrobonja I, Jones S, Abu Kwaik Y. Acquisition of the vacuolar ATPase proton pump and phagosome acidification are essential for escape of *Francisella tularensis* into the macrophage cytosol. Infect Immun 2008;76:2671–2677. [PubMed: 18390995]
15. Chong A, Wehrly TD, Nair V, Fischer ER, Barker JR, Klose KE, Celli J. The early phagosomal stage of *Francisella tularensis* determines optimal phagosomal escape and *Francisella* pathogenicity island protein expression. Infect Immun 2008;76:5488–5499. [PubMed: 18852245]
16. Clemens DL, Lee BY, Horwitz MA. *Francisella tularensis* phagosomal escape does not require acidification of the phagosome. Infect Immun 2009;77:1757–1773. [PubMed: 19237528]

17. Checroun C, Wehrly TD, Fischer ER, Hayes SF, Celli J. Autophagy-mediated reentry of *Francisella tularensis* into the endocytic compartment after cytoplasmic replication. Proc Natl Acad Sci USA 2006;103:14578–14583. [PubMed: 16983090]
18. Santic M, Molmeret M, Barker JR, Klose KE, Dekanic A, Doric M, Abu Kwaik Y. A *Francisella tularensis* pathogenicity island protein essential for bacterial proliferation within the host cell cytosol. Cell Microbiol 2007;9:2391–2403. [PubMed: 17517064]
19. Mohapatra NP, Soni S, Reilly TJ, Liu J, Klose KE, Gunn JS. Combined deletion of four *Francisella novicida* acid phosphatases attenuates virulence and macrophage vacuolar escape. Infect Immun 2008;76:3690–3699. [PubMed: 18490464]
20. Lai XH, Golovliov I, Sjöstedt A. *Francisella tularensis* induces cytopathogenicity and apoptosis in murine macrophages via a mechanism that requires intracellular bacterial multiplication. Infect Immun 2001;69:4691–4694. [PubMed: 11402018]
21. Mariathasan S, Weiss DS, Dixit VM, Monack DM. Innate immunity against *Francisella tularensis* is dependent on the ASC/caspase-1 axis. J Exp Med 2005;202:1043–1049. [PubMed: 16230474]
22. Rajaram MV, Butchar JP, Parsa KV, Cremer TJ, Amer A, Schlesinger LS, Tridandapani S. Akt and SHIP modulate *Francisella* escape from the phagosome and induction of the Fas-mediated death pathway. PLoS One 2009;4:e7919. [PubMed: 19936232]
23. Mougous JD, Cuff ME, Raunser S, Shen A, Zhou M, Gifford CA, Goodman AL, Joachimiak G, Ordoñez CL, Lory S, et al. A virulence locus of *Pseudomonas aeruginosa* encodes a protein secretion apparatus. Science 2006;312:1526–1530. [PubMed: 16763151]
24. Pukatzki S, Ma AT, Sturtevant D, Krastins B, Sarracino D, Nelson WC, Heidelberg JF, Mekalanos JJ. Identification of a conserved bacterial protein secretion system in *Vibrio cholerae* using the *Dictyostelium* host model system. Proc Natl Acad Sci USA 2006;103:1528–1533. [PubMed: 16432199]
25. Meibom KL, Forslund AL, Kuoppa K, Alkhuder K, Dubail I, Dupuis M, Forsberg A, Charbit A. Hfq, a novel pleiotropic regulator of virulence-associated genes in *Francisella tularensis*. Infect Immun 2009;77:1866–1880. [PubMed: 19223477]
26. Baron GS, Nano FE. MglA and MglB are required for the intramacrophage growth of *Francisella novicida*. Mol Microbiol 1998;29:247–259. [PubMed: 9701818]
27. Brotcke A, Monack DM. Identification of fevR, a novel regulator of virulence gene expression in *Francisella novicida*. Infect Immun 2008;76:3473–3480. [PubMed: 18559431]
28. Brotcke A, Weiss DS, Kim CC, Chain P, Malfatti S, Garcia E, Monack DM. Identification of MglA-regulated genes reveals novel virulence factors in *Francisella tularensis*. Infect Immun 2006;74:6642–6655. [PubMed: 17000729]
29. Charity JC, Costante-Hamm MM, Balon EL, Boyd DH, Rubin EJ, Dove SL. Twin RNA polymerase-associated proteins control virulence gene expression in *Francisella tularensis*. PLoS Pathog 2007;3:e84. [PubMed: 17571921]
30. Mohapatra NP, Soni S, Bell BL, Warren R, Ernst RK, Muszynski A, Carlson RW, Gunn JS. Identification of an orphan response regulator required for the virulence of *Francisella* spp. and transcription of pathogenicity island genes. Infect Immun 2007;75:3305–3314. [PubMed: 17452468]
31. Buchan BW, McCaffrey RL, Lindemann SR, Allen LA, Jones BD. Identification of migR, a regulatory element of the *Francisella tularensis* live vaccine strain iglABCD virulence operon required for normal replication and trafficking in macrophages. Infect Immun 2009;77:2517–2529. [PubMed: 19349423]
32. Mohapatra NP, Balagopal A, Soni S, Schlesinger LS, Gunn JS. AcpA is a *Francisella* acid phosphatase that affects intramacrophage survival and virulence. Infect Immun 2007;75:390–396. [PubMed: 17060465]
33. Reilly TJ, Baron GS, Nano FE, Kuhlenschmidt MS. Characterization and sequencing of a respiratory burst-inhibiting acid phosphatase from *Francisella tularensis*. J Biol Chem 1996;271:10973–10983. [PubMed: 8631917]
34. Appelberg R. Neutrophils and intracellular pathogens: beyond phagocytosis and killing. Trends Microbiol 2007;15:87–92. [PubMed: 17157505]
35. Nauseef WM. How human neutrophils kill and degrade microbes: an integrated view. Immunol Rev 2007;219:88–102. [PubMed: 17850484]

36. McCaffrey RL, Allen LA. *Francisella tularensis* LVS evades killing by human neutrophils via inhibition of the respiratory burst and phagosome escape. J Leukoc Biol 2006;80:1224–1230. [PubMed: 16908516]
37. Olakanmi O, Britigan BE, Schlesinger LS. Gallium disrupts iron metabolism of mycobacteria residing within human macrophages. Infect Immun 2000;68:5619–5627. [PubMed: 10992462]
38. Fortier AH, Leiby DA, Narayanan RB, Asafoadjei E, Crawford RM, Nacy CA, Meltzer MS. Growth of *Francisella tularensis* LVS i n macrophages: the acidic intracellular compartment provides essential iron required for growth. Infect Immun 1995;63:1478–1483. [PubMed: 7890413]
39. Clay CD, Soni S, Gunn JS, Schlesinger LS. Evasion of complement-mediated lysis and complement C3 deposition are regulated by *Francisella tularensis* lipopolysaccharide O antigen. J Immunol 2008;181:5568–5578. [PubMed: 18832715]
40. Pierini LM, Eddy RJ, Fuortes M, Seveau S, Casulo C, Maxfield FR. Membrane lipid organization is critical for human neutrophil polarization. J Biol Chem 2003;278:10831–10841. [PubMed: 12522144]
41. Crowther JE, Schlesinger LS. Endocytic pathway for surfactant protein A in human macrophages: binding, clathrin-mediated uptake, and trafficking through the endolysosomal pathway. Am J Physiol Lung Cell Mol Physiol 2006;290:L334–L342. [PubMed: 16169899]
42. Jackson SH, Gallin JI, Holland SM. The p47phox mouse knockout model of chronic granulomatous disease. J Exp Med 1995;182:751–758. [PubMed: 7650482]
43. Parsa KV, Ganesan LP, Rajaram MV, Gavrilin MA, Balagopal A, Mohapatra NP, Wewers MD, Schlesinger LS, Gunn JS, Tridandapani S. Macrophage pro-inflammatory response to *Francisella novicida* infection is regulated by SHIP. PLoS Pathog 2006;2:e71. [PubMed: 16848641]
44. Dang PM, Stensballe A, Boussetta T, Raad H, Dewas C, Kroviarski Y, Hayem G, Jensen ON, Gougerot-Pocidalo MA, El-Benna J. A specific p47phox-serine phosphorylated by convergent MAPKs mediates neutrophil NADPH oxidase priming at inflammatory sites. J Clin Invest 2006;116:2033–2043. [PubMed: 16778989]
45. Rajaram MV, Ganesan LP, Parsa KV, Butchar JP, Gunn JS, Tridandapani S. Akt/Protein kinase B modulates macrophage inflammatory response to *Francisella* infection and confers a survival advantage in mice. J Immunol 2006;177:6317–6324. [PubMed: 17056562]
46. Dang PM, Fontayne A, Hakim J, El Benna J, Périanin A. Protein kinase C zeta phosphorylates a subset of selective sites of the NADPH oxidase component p47phox and participates in formyl peptide-mediated neutrophil respiratory burst. J Immunol 2001;166:1206–1213. [PubMed: 11145703]
47. Felts RL, Reilly TJ, Calcutt MJ, Tanner JJ. Crystallization of a newly discovered histidine acid phosphatase from *Francisella tularensis*. Acta Crystallogr Sect F Struct Biol Cryst Commun 2006;62:32–35.
48. Felts RL, Reilly TJ, Tanner JJ. Crystallization of AcpA, a respiratory burst-inhibiting acid phosphatase from *Francisella tularensis*. Biochim Biophys Acta 2005;1752:107–110. [PubMed: 15935744]
49. Felts RL, Reilly TJ, Tanner JJ. Structure of *Francisella tularensis* AcpA: prototype of a unique superfamily of acid phosphatases and phospholipases C. J Biol Chem 2006;281:30289–30298. [PubMed: 16899453]
50. Reilly TJ, Felts RL, Henzl MT, Calcutt MJ, Tanner JJ. Characterization of recombinant *Francisella tularensis* acid phosphatase A. Protein Expr Purif 2006;45:132–141. [PubMed: 15964202]
51. Schulert GS, McCaffrey RL, Buchan BW, Lindemann SR, Hollenback C, Jones BD, Allen LA. *Francisella tularensis* genes required for inhibition of the neutrophil respiratory burst and intramacrophage growth identified by random transposon mutagenesis of strain LVS. Infect Immun 2009;77:1324–1326. [PubMed: 19204089]
52. Aguirre-García MM, Okhuysen PC. *Cryptosporidium parvum*: identification and characterization of an acid phosphatase. Parasitol Res 2007;101:85–89. [PubMed: 17252269]
53. Hartland EL, Green SP, Phillips WA, Robins-Browne RM. Essential role of YopD in inhibition of the respiratory burst of macrophages by *Yersinia enterocolitica*. Infect Immun 1994;62:4445–4453. [PubMed: 7927708]

54. Gallois A, Klein JR, Allen LA, Jones BD, Nauseef WM. *Salmonella* pathogenicity island 2-encoded type III secretion system mediates exclusion of NADPH oxidase assembly from the phagosomal membrane. J Immunol 2001;166:5741–5748. [PubMed: 11313417]
55. Baca OG, Roman MJ, Glew RH, Christner RF, Buhler JE, Aragon AS. Acid phosphatase activity in *Coxiella burnetii*: a possible virulence factor. Infect Immun 1993;61:4232–4239. [PubMed: 8406811]
56. Lindgren H, Stenmark S, Chen W, Tärnvik A, Sjöstedt A. Distinct roles of reactive nitrogen and oxygen species to control infection with the facultative intracellular bacterium *Francisella tularensis*. Infect Immun 2004;72:7172–7182. [PubMed: 15557642]
57. Heyworth PG, Curnutte JT, Nauseef WM, Volpp BD, Pearson DW, Rosen H, Clark RA. Neutrophil nicotinamide adenine dinucleotide phosphate oxidase assembly. Translocation of p47-phox and p67-phox requires interaction between p47-phox and cytochrome b558. J Clin Invest 1991;87:352–356. [PubMed: 1985107]
58. Volpp BD, Nauseef WM, Clark RA. Two cytosolic neutrophil oxidase components absent in autosomal chronic granulomatous disease. Science 1988;242:1295–1297. [PubMed: 2848318]
59. Chen Q, Powell DW, Rane MJ, Singh S, Butt W, Klein JB, McLeish KR. Akt phosphorylates p47phox and mediates respiratory burst activity in human neutrophils. J Immunol 2003;170:5302–5308. [PubMed: 12734380]
60. Fontayne A, Dang PM, Gougerot-Pocidalo MA, El-Benna J. Phosphorylation of p47phox sites by PKC alpha, beta II, delta, and zeta: effect on binding to p22phox and on NADPH oxidase activation. Biochemistry 2002;41:7743–7750. [PubMed: 12056906]
61. Torres M. Mitogen-activated protein kinase pathways in redox signaling. Front Biosci 2003;8:d369–d391. [PubMed: 12456373]
62. Torres M, Forman HJ. Redox signaling and the MAP kinase pathways. Biofactors 2003;17:287–296. [PubMed: 12897450]
63. Wang Y, Zeigler MM, Lam GK, Hunter MG, Eubank TD, Khramtsov VV, Tridandapani S, Sen CK, Marsh CB. The role of the NADPH oxidase complex, p38 MAPK, and Akt in regulating human monocyte/macrophage survival. Am J Respir Cell Mol Biol 2007;36:68–77. [PubMed: 16931806]
64. Babior BM. The leukocyte NADPH oxidase. Isr Med Assoc J 2002;4:1023–1024. [PubMed: 12489496]
65. Brown GE, Stewart MQ, Liu H, Ha VL, Yaffe MB. A novel assay system implicates PtdIns(3,4)P (2), PtdIns(3)P, and PKC delta in intracellular production of reactive oxygen species by the NADPH oxidase. Mol Cell 2003;11:35–47. [PubMed: 12535519]
66. El-Benna J, Dang PM, Gougerot-Pocidalo MA. Priming of the neutrophil NADPH oxidase activation: role of p47phox phosphorylation and NOX2 mobilization to the plasma membrane. Semin Immunopathol 2008;30:279–289. [PubMed: 18536919]
67. Bokoch GM, Diebold BA. Current molecular models for NADPH oxidase regulation by Rac GTPase. Blood 2002;100:2692–2696. [PubMed: 12351373]
68. Lodge R, Descoteaux A. Phagocytosis of *Leishmania donovani amastigotes* is Rac1 dependent and occurs in the absence of NADPH oxidase activation. Eur J Immunol 2006;36:2735–2744. [PubMed: 16955522]
69. Lodge R, Diallo TO, Descoteaux A. *Leishmania donovani* lipophosphoglycan blocks NADPH oxidase assembly at the phagosome membrane. Cell Microbiol 2006;8:1922–1931. [PubMed: 16848789]
70. Vázquez-Torres A, Fantuzzi G, Edwards CK 3rd, Dinarello CA, Fang FC. Defective localization of the NADPH phagocyte oxidase to *Salmonella*-containing phagosomes in tumor necrosis factor p55 receptor-deficient macrophages. Proc Natl Acad Sci USA 2001;98:2561–2565. [PubMed: 11226278]
71. Vazquez-Torres A, Jones-Carson J, Mastroeni P, Ischiropoulos H, Fang FC. Antimicrobial actions of the NADPH phagocyte oxidase and inducible nitric oxide synthase in experimental salmonellosis. I. Effects on microbial killing by activated peritoneal macrophages in vitro. J Exp Med 2000;192:227–236. [PubMed: 10899909]
72. Vazquez-Torres A, Xu Y, Jones-Carson J, Holden DW, Lucia SM, Dinauer MC, Mastroeni P, Fang FC. *Salmonella* pathogenicity island 2-dependent evasion of the phagocyte NADPH oxidase. Science 2000;287:1655–1658. [PubMed: 10698741]

73. Allen LA, Allgood JA, Han X, Wittine LM. Phosphoinositide3-kinase regulates actin polymerization during delayed phagocytosis of *Helicobacter pylori*. J Leukoc Biol 2005;78:220–230. [PubMed: 15809290]

74. Allen LA, Beecher BR, Lynch JT, Rohner OV, Wittine LM. *Helicobacter pylori* disrupts NADPH oxidase targeting in human neutrophils to induce extracellular superoxide release. J Immunol 2005;174:3658–3667. [PubMed: 15749904]

75. DeLeo FR, Allen LA, Apicella M, Nauseef WM. NADPH oxidase activation and assembly during phagocytosis. J Immunol 1999;163:6732–6740. [PubMed: 10586071]

76. Child R, Wehrly TD, Rockx-Brouwer D, Dorward DW, Celli J. Acid phosphatases do not contribute to the pathogenesis of type A *Francisella tularensis*. Infect Immun 2010;78:59–67. [PubMed: 19858304]

77. Aragon V, Kurtz S, Flieger A, Neumeister B, Cianciotto NP. Secreted enzymatic activities of wild-type and pilD-deficient *Legionella pneumophila*. Infect Immun 2000;68:1855–1863. [PubMed: 10722574]

78. Santic M, Molmeret M, Abu Kwaik Y. Modulation of biogenesis of the *Francisella tularensis* subsp. *novicida*-containing phagosome in quiescent human macrophages and its maturation into a phagolysosome upon activation by IFN-gamma. Cell Microbiol 2005;7:957–967. [PubMed: 15953028]

Abbreviations used in this paper

ΔABCH	deletion of acid phosphatases AcpA, AcpB, AcpC, and Hap
Acp	acid phosphatase
BMDM	bone marrow-derived macrophage
DPI	diphenylene iodonium
FN	*Francisella novicida*
FKFN	formalin-killed *Francisella novicida*
FKFT	formalin-killed *Francisella tularensis*
FPI	*Francisella* pathogenicity island
LVS	live vaccine strain
MDM	monocyte-derived macrophage
MOI	multiplicity of infection
OPZ	serum-opsonized zymosan
PKC	protein kinase C
PMN	polymorphonuclear leukocyte
ROS	reactive oxygen species
SchuS4	*F. tularensis* subspecies *tularensis* SchuS4
WT	wild-type

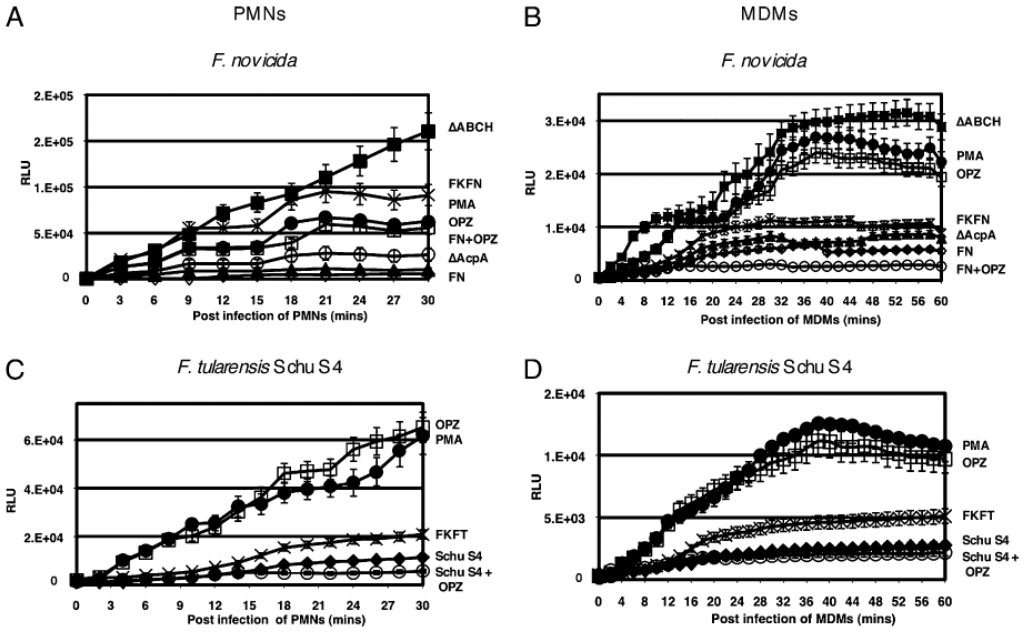

FIGURE 1.

Detection of ROS production in human neutrophils and MDMs. The luminescence was measured over a 30-min (*A*, *C*, neutrophils) or 60-min (*B*, *D*, MDMs) time period in these human phagocytes, and the baseline ROS luminescence was determined by measuring the luminescence of control cells treated with medium only. *A* and *B*, *F. novicida* (FN; ◊), Δ*acpA* (▲), ΔABCH (■), formalin-killed *F. novicida* (FKFN; X), and *F. novicida* followed by serum-opsonized zymosan (FN+OPZ; ○), serum-opsonized zymosan (OPZ; □), or 200 nM PMA (●). *C* and *D*, *F. tularensis* subspecies *tularensis* SchuS4 (Schu S4; ◆), formalin-killed *F. tularensis* subspecies *tularensis* (FKFT; X), and *F. tularensis* subspecies *tularensis* followed by serum-opsonized zymosan (Schu S4 + OPZ; ○), serum-opsonized zymosan (OPZ; □), or 200 nM PMA (●). Data are the mean ± SD of triplicate samples from a representative experiment ($n = 7$).

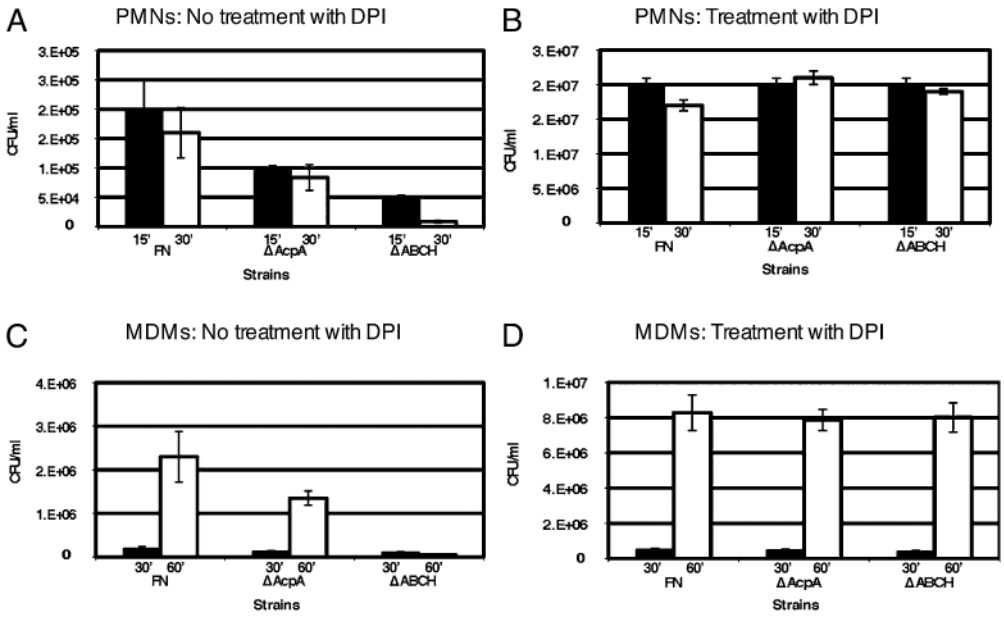

FIGURE 2.

Intracellular survival assays performed in neutrophils or MDMs in the absence or presence of DPI (10 μM). Macrophages were infected with *F. novicida* or the mutant derivatives Δ*acpA* or ΔABCH in the absence (*A, C*) or presence (*B, D*) of DPI (10 μM). Black bars represent 15 min in neutrophils (*A, B*) and 30 min in MDMs (*C, D*), and white bars represent 30 min in neutrophils (*A, B*) and 60 min postinfection in MDMs (*C, D*). Data are the mean ± SD of triplicate samples from one representative experiment ($n = 5$).

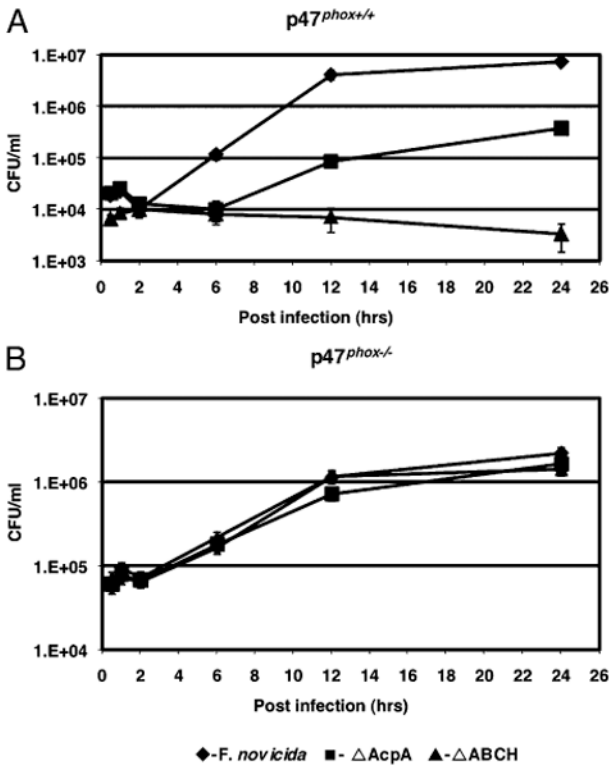

FIGURE 3.

Intramacrophage survival of *F. novicida* acid phosphatase mutants in BMDMs from p47$^{phox+/+}$ and p47$^{phox-/-}$ knockout mice. BMDMs were isolated from p47$^{phox+/+}$ WT C57BL/J mice (*A*) and p47$^{phox-/-}$ knockout mice C57BL/J (*B*) infected with *F. novicida* or the mutant derivatives *acpA* or ΔABCH. Data are the mean ± SD of triplicate samples from one representative experiment (n = 3).

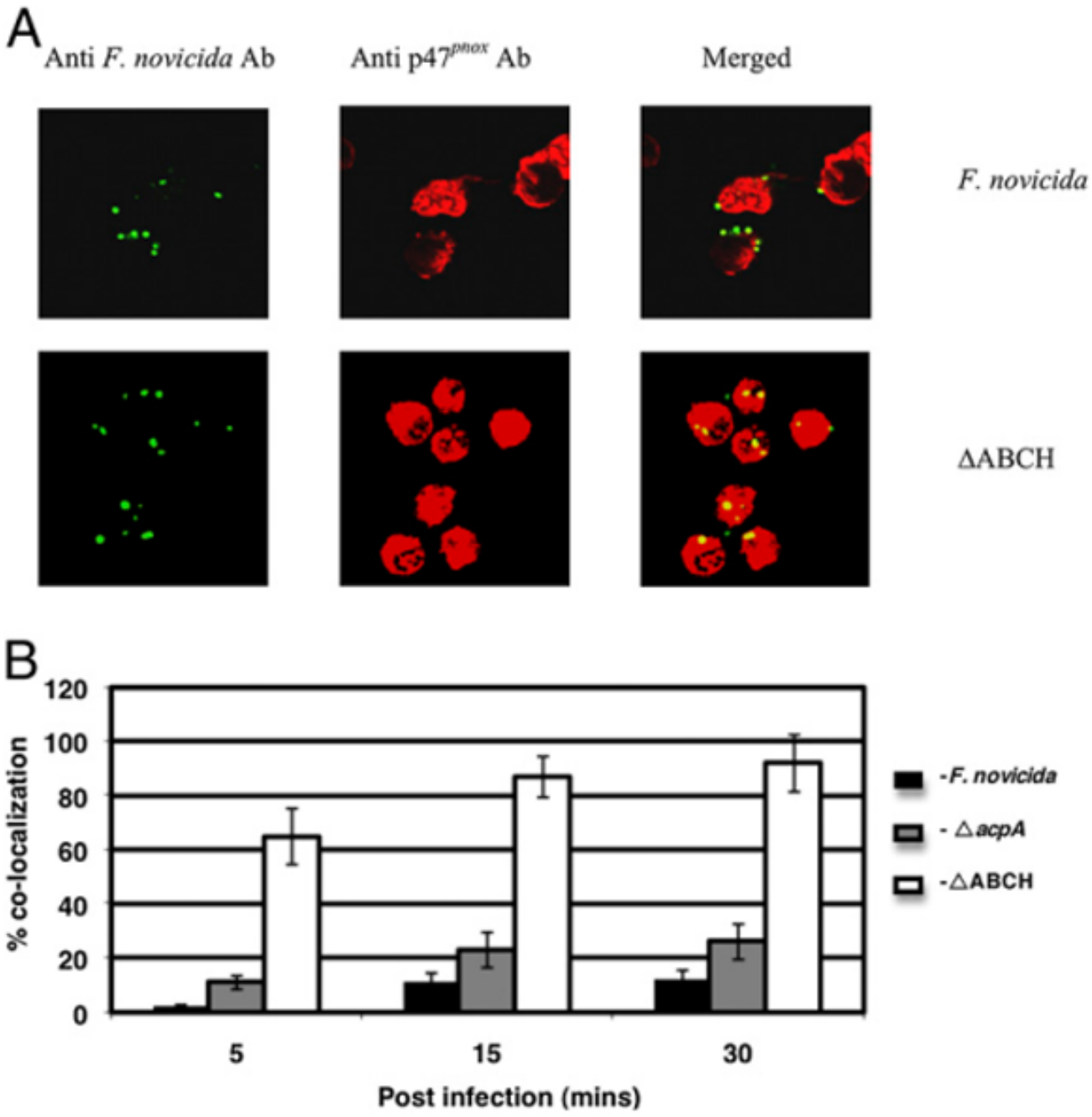

FIGURE 4.

Colocalization of the *F. novicida* WT strain and mutant strains with p47^{phox} in neutrophils. *A*, Colocalization of the *F. novicida* WT and ΔABCH or Δ*acpA* mutant strains with p47^{phox} was determined at 5, 15, and 30 min postinfection in neutrophils. *Francisella* was detected following staining with goat anti-mouse Alexa Fluor 488 (green color), and p47^{phox} was detected following staining with donkey anti-rabbit Alexa Fluor 546 (red color). Representative confocal microscopy images of *F. novicida* and ΔABCH colocalized with p47^{phox} within neutrophils are shown at 30 min postinfection. The images are representative of 1000 infected cells examined from triplicate coverslips in three independent experiments. Original magnification ×63. *B*, Colocalization of the *F. novicida* WT, Δ*acpA*, and ΔABCH mutant

strains with p47^{phox} was quantified at 5, 15, and 30 min postinfection. Analyses were based on examination of 1000 infected cells examined from triplicate coverslips in three independent experiments. The results shown are cumulative data of three experiments (mean ± SD of nine samples; triplicate samples were included in each test group in each experiment).

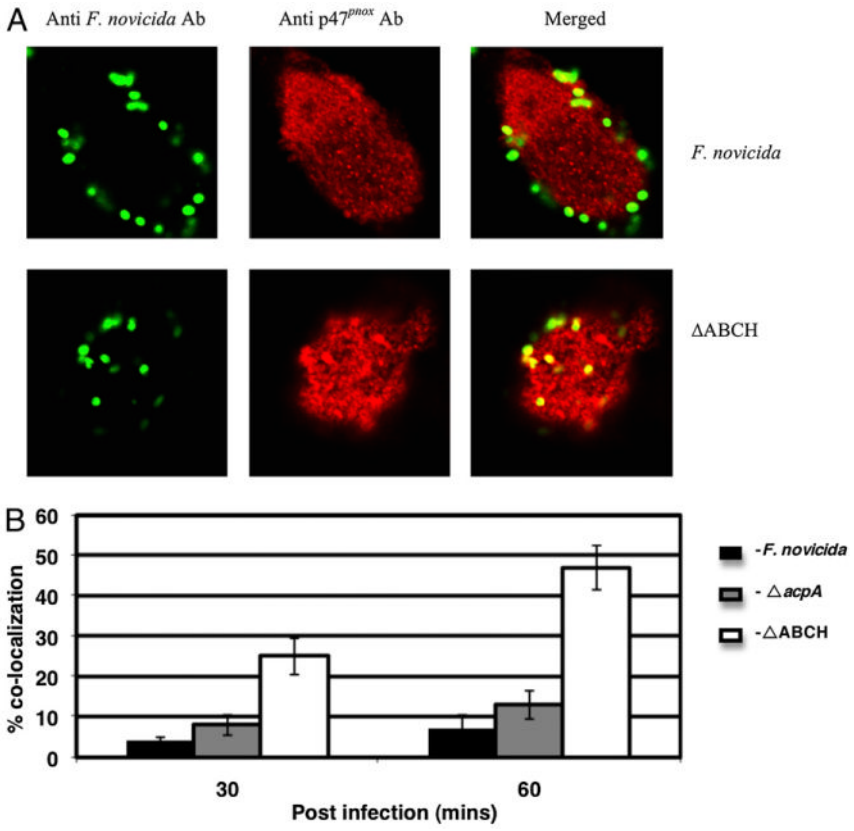

FIGURE 5.

Colocalization of the *F. novicida* WT strain and mutant strains with p47^{phox} in macrophages. *A*, Colocalization of the *F. novicida* WT and ΔABCH or Δ*acpA* mutant strains with p47^{phox} was determined at 30 and 60 min post-infection in MDMs. *Francisella* was detected following staining with goat anti-mouse Alexa Fluor 488 (green color), and p47^{phox} was detected following staining with donkey anti-rabbit Alexa Fluor 546 (red color). Representative confocal microscopy images of *F. novicida* and ΔABCH colocalized with p47^{phox} within MDMs are shown 60 min postinfection. The images are representative of 1000 infected cells examined from triplicate coverslips in three independent experiments. Original magnification ×63. *B*, Colocalization of the *F. novicida* WT, Δ*acpA*, and ΔABCH mutant strains with p47^{phox} was quantified at 30 and 60 min postinfection. Analyses were based on examination of 1000 infected cells examined from triplicate coverslips in three independent experiments. The results shown are cumulative data of three experiments (mean ± SD of nine samples; triplicate samples were included in each test group in each experiment).

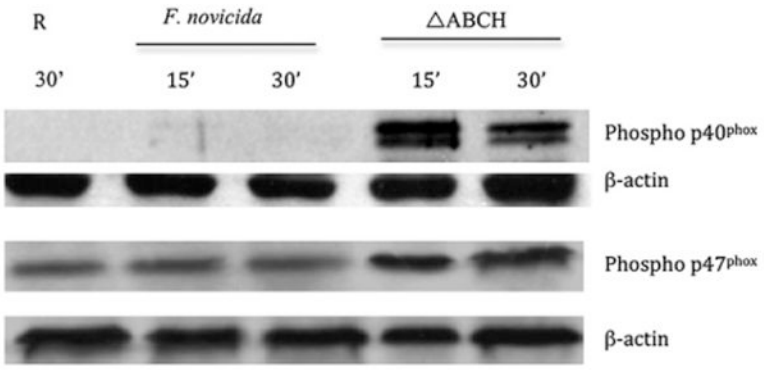

FIGURE 6.

The effect of *F. novicida* WT and *acp* mutants on phosphorylation of p47^{phox} and p40^{phox} in neutrophils. Neutrophils were incubated with *F. novicida* WT or ΔABCH strains for the times shown. Lysates were loaded by protein equivalents, separated by SDS-PAGE, and analyzed by Western blotting with Abs specific for phosphorylated p47^{phox} (rabbit anti-Pp47^{phox}) and phosphorylated p40^{phox} (rabbit anti-Pp40^{phox}). The same membrane was reprobed with β-actin Ab to verify equal protein loading. Resting (R) represents the uninfected PMN cell lysates collected at 30 min postinfection. A representative Western blot image is shown (n = 7).

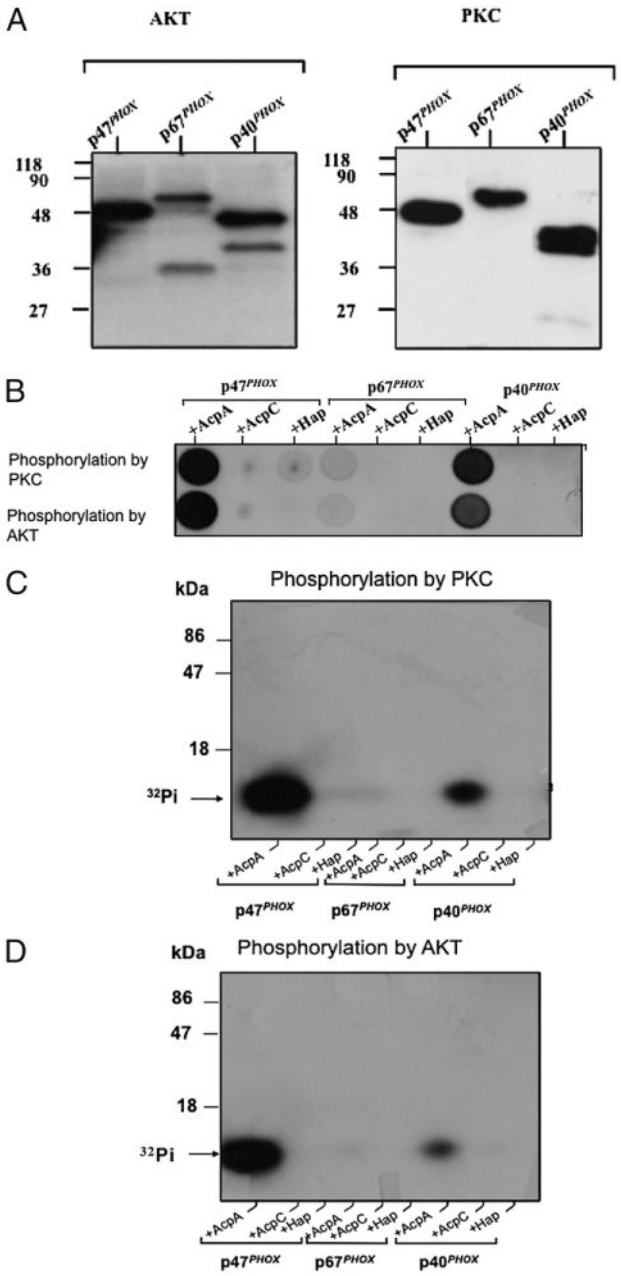

FIGURE 7.

The effect of *F. novicida* Acps on phosphorylation of p40^{phox} and p47^{phox} in vitro. *A*, Phosphorylation of p47^{phox}, p67^{phox}, and p40^{phox} by AKT and PKC. Recombinant p47^{phox}, p67^{phox}, and p40^{phox} (5 μg each) were phosphorylated by active PKC or Akt in the presence of 1 μCi of [^{32}P]-[γ]g-ATP for 30 min. The reaction was terminated by adding the same volume of 2× Laemmli sample buffer, and the proteins were separated by SDS-PAGE and transferred to a nitrocellulose membrane. The proteins were stained by ponceau red (data not shown), and [^{32}P]-labeled p47^{phox}, p67^{phox}, and p40^{phox} were detected by phosphoimaging and autoradiography. *B*, Dot blot of released [^{32}Pi]. The nitrocellulose area containing [^{32}P]-labeled p47^{phox}, p67^{phox}, and p40^{phox} was cut and incubated for 30 min at 37°C with polyvinylpyrrolidone, washed, and then incubated with the different purified acid phosphatases. Supernatants containing released [^{32}P] were spotted onto a thin-layer cellulose

plate and detected by autoradiography. *C* and *D*, Confirmation of release of [^{32}Pi]. To confirm that the above signal was not due to the release of proteins from the nitrocellulose, the supernatant was subjected to 15% SDS-PAGE and analyzed by autoradiography. *C*, Phosphorylation by PKC. *D*, Phosphorylation by Akt.